

Angular Distribution of Neutrons Scattered from Aluminum, Iron, and Lead*

W. D. WHITEHEAD AND S. C. SNOWDON

Bartol Research Foundation of the Franklin Institute, Swarthmore, Pennsylvania

(Received May 29, 1953)

The differential cross sections for the scattering of 3.7-Mev neutrons from aluminum, iron, and lead have been measured in a ring geometry using a molded Lucite-zinc sulfide button as a detector. The measurements were taken over an angular range of 127 degrees between 13 degrees and 140 degrees with an angular resolution better than ± 10 degrees. Effects due to higher-order scattering in the scatterer were removed by extrapolation.

INTRODUCTION

MEASUREMENTS of the angular distribution of fast neutrons scattered from a large number of elements have been reported previously by Kikuchi *et al.*,¹ and Amaldi *et al.*² in which the main features of the distribution could be explained as the diffraction effects due to the scattering of neutron waves by spherical particles. More recently Remund and Ricamo³ have measured angular distribution of 3.7-Mev neutrons scattered from carbon while Walt and Barschall,⁴ using 1.00-Mev neutrons have reported the angular distributions for a large number of elements. Feshbach, Porter, and Weisskopf,⁵ using a modification of the continuum theory of nuclear reactions, have reproduced the average features of the total neutron cross section *vs* energy and atomic number as measured by Barschall.⁶ Feshbach, Porter, and Weisskopf⁷ have also computed the angular distributions of elastically scattered neutrons using this same modification of the continuum theory and the

general features agree rather well with the measurements of Walt and Barschall.⁴ Our measurements on aluminum, iron and lead, using 3.7-Mev neutrons, were undertaken with the thought that the angular distribution in this energy range would be of value in view of the present theoretical considerations.

EXPERIMENTAL

Figure 1 shows the experimental arrangement that was used to measure the angular distribution of neutrons scattered from aluminum, iron, and lead. The source of neutrons is a chamber of deuterium gas at 0.5 atmosphere and 2.0 cm in depth bombarded with about 10 microamperes of 1.0-Mev deuterons which, after passing through the nickel foil and gas, have a mean energy of about 0.65 Mev. These neutrons are detected by a pressure molded Lucite-zinc sulfide button⁸ mounted directly on the face of an RCA 5819 photomultiplier. The direct beam is cut out by a suitably tapered 10-inch long, 1 $\frac{1}{8}$ -inch diameter iron cylinder. The scatterer was chosen to have the shape of a ring in order to increase as much as possible the number of scattered neutrons. The scattering angle θ is varied by moving the scattering rings laterally and by using rings of various sizes. For angles between 52° and 140°, 8-inch o.d. rings were used with a mean source-detector distance R_0 of 40 cm. For θ between 24° and 52°, 6-inch o.d. rings were used with R_0 equal to 60 cm. For the point at 13°, 4-in. o.d. rings were used with R_0 equal to 72 cm.

In order to discuss the measurements that must be made to arrive at the differential scattering cross section, it is convenient to define several quantities. For a given number of neutrons emitted by the neutron source, let N_S be the number of neutrons recorded by the detector with the scatterer and direct beam attenuator in place. Let N_B be the number of neutrons detected with the scatterer removed and let N_D be the number of neutrons recorded with the scatterer and attenuator removed. $N_S - N_B$ is the number of scattered neutrons recorded by the detector that originate in the source, and $N_D - N_B$ is the number of neutrons direct from the source that are recorded by the detector. Let

⁸ W. F. Hornyak, *Rev. Sci. Instr.* **23**, 264 (1952). The authors are indebted to Dr. Hornyak for supplying them with a Lucite-zinc sulfide molded button.

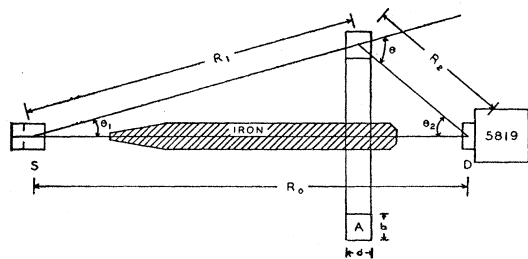


FIG. 1. Ring geometry for scatterer (S), deuterium gas at one-half atmosphere pressure to give neutrons of about 3.7 Mev; (D) Lucite-zinc sulfide scintillation detector; (A) ring scatterer of rectangular cross section.

* Assisted by the joint program of the U. S. Office of Naval Research and the U. S. Atomic Energy Commission.

¹ Kikuchi, Aoki, and Wakatuki, *Proc. Phys. Math. Soc. Japan* **21**, 410 (1939); T. Wakatuki and S. Kikuchi, *Proc. Phys. Math. Soc. Japan* **21**, 656 (1939); T. Wakatuki, *Proc. Phys. Math. Soc. Japan* **22**, 430 (1940).

² Amaldi, Bocciarelli, Cacciapuoti, and Trabacchi, *International Conference on Fundamental Particles and Low Temperature* (The Physical Society, London, 1947), Vol. 1.

³ A. E. Remund and R. Ricamo, *Helv. Phys. Acta* **25**, 441 (1952).

⁴ M. Walt and H. H. Barschall, *Phys. Rev.* **90**, 714 (1953).

⁵ Feshbach, Porter, and Weisskopf, *Phys. Rev.* **90**, 166 (1953).

⁶ H. H. Barschall, *Phys. Rev.* **86**, 431 (1952); Miller, Adair, Bockelman, and Darden, *Phys. Rev.* **88**, 83 (1952).

⁷ Feshbach, Porter, and Weisskopf, *Bull. Am. Phys. Soc.* **28**, No. 3, 29 (1953).

the scattering ratio be defined as

$$S \equiv (N_S - N_B) / (N_D - N_B).$$

Appendix I then shows that the scattering ratio S is related to the apparent differential scattering cross section $\bar{\sigma}(\theta)$ through the relation

$$S = [I(\theta_1)/I(0)] \cdot [R_0^2/R_1^2 R_2^2] \cdot \bar{\sigma}(\theta) A(\theta_2) E(E_n) n V F(\theta_2) \exp(-\sigma n d), \quad (1)$$

where $I(\theta_1)$ is the number of neutrons emitted from the source per steradian per unit monitor flux, $A(\theta_2)$ is the angular sensitivity of the neutron detector normalized to unity at zero angle, $E(E_n)$ is the energy sensitivity of the neutron detector normalized to unity for the energy of the direct beam, nV is the number of scattering nuclei, σ is the total scattering cross section, and $F(\theta_2)$ is an attenuation factor which is defined more fully in Appendix I.

In general, the scattering ratio S is made up of a sum of terms $S = S_1 + S_2 + \text{etc.}$, where $S_1, S_2, \text{etc.}$ refer to the neutrons scattered into the detector by single scattering, double scattering, etc. Thus, $\bar{\sigma}(\theta)$ is simply a measure of the differential scattering cross section, assuming that all neutrons are singly scattered, since $\bar{\sigma}(\theta)$ becomes exactly $\sigma(\theta)$ if S is replaced by S_1 . In order to separate the components $S_1, S_2, \text{etc.}$, one measures the scattering ratio S for a fixed angle θ as a function of the axial thickness of the ring scatterer d . The value of $\sigma(\theta)$ at $d=0$ is then the average differential scattering cross section for all scattered neutrons (elastic and inelastic) weighted according to the energy-sensitivity of the detector $E(E_n)$. In the ideal case, if the energy-sensitivity curve adequately discriminates against the inelastically scattered neutrons, the above value of $\bar{\sigma}(\theta)$ for $d=0$ becomes the differential cross section for elastic scattering $\sigma(\theta)$.

In order to measure $\bar{\sigma}(\theta)$ it is necessary to consider the following factors.

1. *Energy resolution of incident neutrons.*—The mean energy of the neutrons incident on the scatterer varies between 3.70 Mev and 3.74 Mev depending on the angle θ_1 . The energy spread in the beam due to target thickness and voltage stability of the generator is about 200 kev.

2. *Neutron flux monitor.*—A proportional counter filled with one atmosphere of butane was placed very close to the target chamber at 90 degrees with respect to the source-detector axis. The discriminator was set to reject those neutrons that were produced from the $C^{12}(d, n)$ reaction in the vicinity of the magnet box. Actually some difficulty was experienced in obtaining a constant direct-beam neutron count per unit monitor count after the target chamber was just filled with deuterium. The pattern of change, however, was similar in each case and seemed to indicate that some of the deuterium gas was absorbed into the walls of the

chamber. After about an hour or two a ratio was obtained that was constant to ± 5 percent.

3. *Measurement of S .*—In general the direct beam count was about 15–100 times the scattered beam count and the attenuated direct beam count varied from 40 percent to 90 percent of the scattered beam count, each depending on the size and position of the scatterer.

4. *Spacial distribution of neutron source.*—The $N_D - N_B$ count exhibited within a few percent an inverse square variation with distance from the target chamber.

5. *Angular variation of the neutron flux from the D–D reaction, $I(\theta_1)/I(0)$.*—This quantity was computed from the data published by Hunter and Richards.⁹

6. *Measurement of nV , the number of scattering nuclei.*—Each scatterer was weighed on a suitable balance to about one percent accuracy.

7. *Angular variation in sensitivity of the neutron detector, $A(\theta_2)$.*—This quantity varied by about 25 percent over the range of θ_2 used in this experiment. The value of $A(\theta_2)$ was measured to within about 5 percent by rotating the detector about an axis through the detector perpendicular to the source-detector axis.

8. *Measurement of the total cross section.*—This was measured by using $1\frac{1}{8}$ -inch diameter, 1-inch long cylinders of aluminum, iron, and lead. The cross sections obtained for $E_n = 3.7$ Mev were $\sigma(\text{Al}) = 2.55$ barns, $\sigma(\text{Fe}) = 3.51$ barns, and $\sigma(\text{Pb}) = 7.60$ barns each in agreement with the values obtained by Nereson and Darden.¹⁰ The scattering-in corrections were 0.75, 2.4, and 4.3 percent, respectively, for Al, Fe, and Pb, and were obtained from our measurements of the differential cross section.

9. *The attenuation factor F .*—This factor varied from unity by as much as 14 percent depending on the size and shape of the scatterer. This quantity is discussed briefly in Appendix I and a graph of its variation is given in Fig. 2.

10. *Geometrical measurements.*—Measurements of distance were carried out to about ± 1 millimeter. The consequent calculation of mean angles is thus accurate to about one percent. However, because of the finite size of the detector (1 inch diameter, $\frac{5}{8}$ inch height) and the finite size of the scatterers, the detected neutrons are received over a range of angles of about ± 10 degrees in the worst case near $\theta = 90$ degrees.

11. *Variation of the sensitivity of the detector with neutron energy.*—This was measured by comparing our measurement of the angular distribution of neutrons from the D–D reaction with those of Hunter and Richards,⁹ the discrepancy being ascribed to a non-uniform efficiency in our detector. As may be seen in Fig. 3, the sensitivity only drops off slowly with decreasing neutron energy, decreasing by 40 percent in 1 Mev. Since it is desired to discriminate against neutrons that have lost more than 200 kev, this consti-

⁹ G. T. Hunter and H. T. Richards, Phys. Rev. 76, 1445 (1949).

¹⁰ N. Nereson and S. Darden, Phys. Rev. 89, 775 (1953).

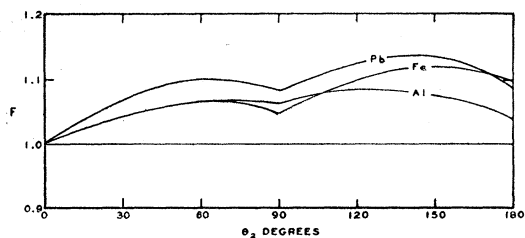


FIG. 2. Attenuation factor F . This quantity is defined in Appendix I. $F \exp(-\sigma nd)$ essentially measures the attenuation of the direct beam into the scatterer times the attenuation of the scattered beam out of the scatterer. The dimensions are for aluminum, iron, and lead: $b=2.54$ cm, 2.54 cm, and 2.54 cm; $d=3.15$ cm, 2.54 cm, and 3.00 cm. The factor F is not shown for the thinner rings used in the experiment.

tutes a serious objection to the use of the Lucite-zinc sulfide detector in this experiment. However, if the inelastically scattered neutrons are more uniformly distributed in angle than the elastically scattered neutrons, then the general features of the differential cross section for elastic scattering will still be evident. In any case the value obtained for $\sigma(\theta)$ must be such that the total cross section achieved by integrating $\sigma(\theta)$ is less than the measured total cross section. That this is the case will be shown later.

12. *Sensitivity of counter to gamma rays.*—Neutron detector must not count the gamma rays resulting from the inelastic scattering of neutrons. An ampoule containing 0.1 milligram of radium was placed directly on the Lucite-zinc sulfide detector and gave a negligible counting rate (less than 1 count in 100 seconds).

13. *Higher-order scattering.*—Appendix II gives an account of the method used in this experiment to allow for double scattering. Essentially it involves placing an upper and lower bound on the possible values of $\sigma(\theta)$ for an observed sequence of values of $\bar{\sigma}(\theta)$ as a function of the axial thickness of the ring. The first calculation estimates the nature of the variation of $\bar{\sigma}(\theta)$ with d/a under the assumption of isotropic scattering. This is given by Eq. (13) which, after comparing with Fig. 4, is

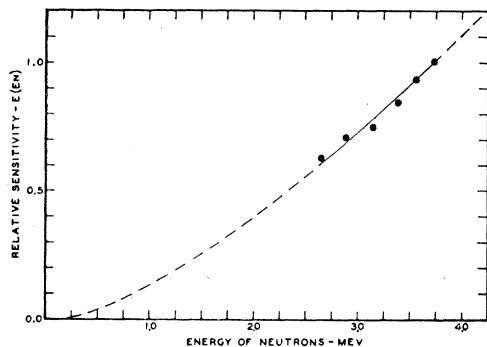


FIG. 3. Energy sensitivity of neutron detector. $E(E_n)$ measures the sensitivity of the neutron detector normalized to unity at 3.7 Mev. Solid circles were measured by us. The dotted curve was obtained from reference 9 by normalizing the two sets of data over the region common to both.

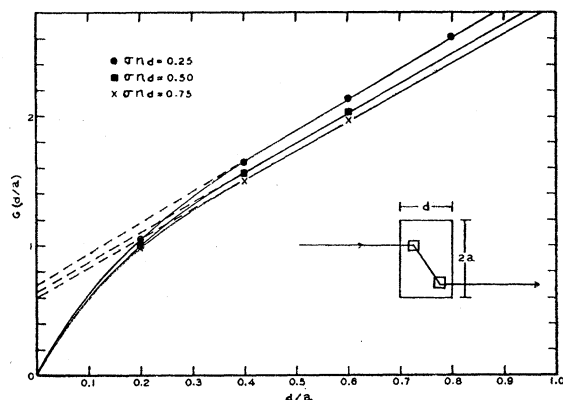


FIG. 4. Variation of straight-through double scattering in a right circular cylinder. The differential cross section was assumed to be isotropic. Specifically this curve is a plot of the function G as defined in Appendix II.

seen to reduce to the practical formula

$$\bar{\sigma}(\theta) = \bar{\sigma}_0(\theta) - 0.282\bar{\sigma}'(\theta), \quad (2)$$

where $\bar{\sigma}_0(\theta)$ is the intercept at $d/a=0$ of the linear portion of the curve and $\bar{\sigma}'(\theta)$ is the slope of the $\bar{\sigma}(\theta)$ vs d/a curve in the linear portion.

The second calculation states that, if the angular distribution is peaked strongly forward, then one expects that the double scattering contribution will cause $\bar{\sigma}(\theta)$ to be a linear function of d or d/a . In this case $\bar{\sigma}_0(\theta)$ is the true differential scattering cross section. Both of these extrapolations are presented on the graphs.

If triple scattering is present, then $\bar{\sigma}(\theta)$ should be a quadratic function of d or d/a for the case in which there is a strong forward peaking of the scattering. Figure 5, for the case of iron, shows some indication of the presence of triple scattering; however, the experimental uncertainty is too large to consider this definite. No attempt was made to remove the triple scattering contributions.

A typical run of data was made as follows: (1) direct beam; (2) attenuated beam; (3) scattered beam from one of the rings for all values of the scattering angle; (4) attenuated beam; (5) direct beam. If the two

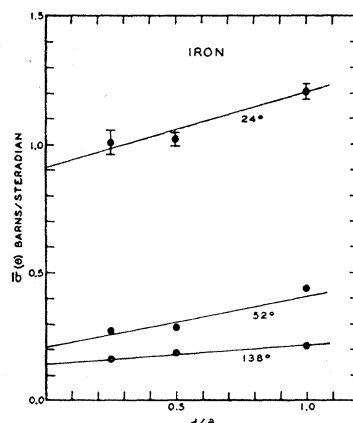


FIG. 5. Apparent differential cross section of iron vs thickness of ring scatterer for three different scattering angles. The thickness is measured relative to a quantity a , which we have taken to be equal to the radial width of the ring in order to establish a correspondence between the ring scatterer and the right circular cylinder scatterer.

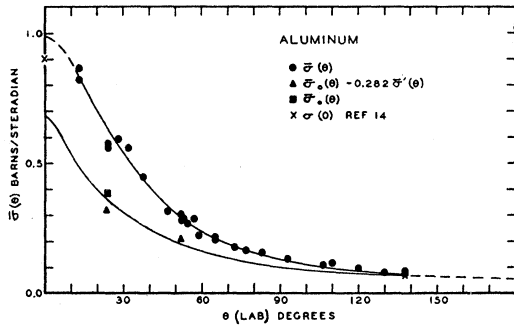


FIG. 6. Angular distribution of 3.7-Mev neutrons scattered from aluminum. $\bar{\sigma}(\theta)$ is apparent differential cross section as defined in the text. $\bar{\sigma}_0(\theta)$ is the differential cross section using a linear extrapolation to remove higher-order scatters. $\bar{\sigma}_0(\theta) - 0.282\sigma'(\theta)$ is the differential cross section in which the higher-order scatters are removed using the isotropic scattering assumption. $\sigma(0)$ is taken from the "Final Report of the Fast Neutron Data Project," U. S. Atomic Energy Commission, NYO-636 (unpublished), in which the nuclear radii were found from our measured values of the total cross section.

values of the direct beam determination differed by more than 10 percent, the data were discarded.

DATA

Figures 6-8 show the experimental points of the apparent differential cross section for 3.7-Mev neutrons incident on aluminum, iron, and lead as calculated from Eq. (1). Only a limited number of angles were chosen in order to determine the effects of higher-order scattering. Figure 5 shows the variation of $\bar{\sigma}(\theta)$ as a function of the ring thickness for the case of iron. In the same manner, similar curves were obtained for lead and aluminum. The extrapolations both for isotropic scattering and forward peaked scattering are shown in Figs. 6, 7, and 8 where a curve is drawn through the points thought to be the appropriate differential cross section, $\sigma(\theta)$ for each case. The total cross sections corresponding to $\sigma(\theta)$ have been calculated and are presented together with the previously measured total cross sections¹⁰ in Table I. It will be noted that the

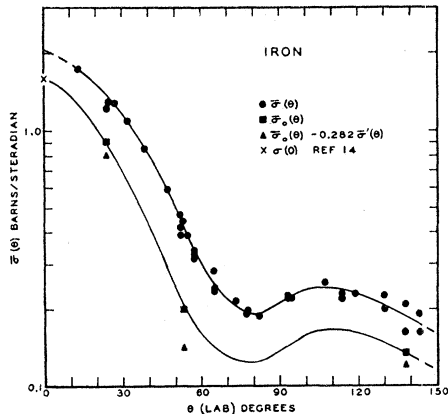


FIG. 7. Angular distribution of 3.7-Mev neutrons scattered from iron. Other remarks in caption of Fig. 6 apply here also.

TABLE I. Total cross sections. Subject to the reservations in the text, the value of $\int \sigma(\theta) d\Omega_\theta$ is the total elastic cross section.

Element	σ_{tot} (meas.) in barns		$\int \sigma(\theta) d\Omega_\theta$ (barns)
	This expt.	Ref. 10	
Aluminum	2.55	2.50	1.73
Iron	3.51	3.55	2.94
Lead	7.60	7.70	5.17

integrated differential cross sections in each case are less than the measured total cross section. The total inelastic cross section cannot be obtained as the difference between the two former cross sections since the measurement of the differential cross section did not discriminate adequately against the inelastically scattered neutrons. However, this subtraction can be carried out approximately if one accepts the following rather crude estimate of the inelastic contribution to $\sigma(\theta)$. There are seven levels in aluminum that can be excited by 3.7-Mev neutrons.¹¹ If we assume that the maximum total inelastic cross section is about 50 percent of the total cross section and that the seven levels in aluminum are equally excited, then the inelastic neutrons contribute less than 15 percent to the total cross sections corresponding to $\sigma(\theta)$. Similar arguments using the known levels in iron and lead show that the inelastic contribution in these elements is less than 20 percent.

In conclusion, the authors wish to express their appreciation to Dr. W. F. G. Swann, Director of The Bartol Research Foundation, for his sustained interest in this problem.

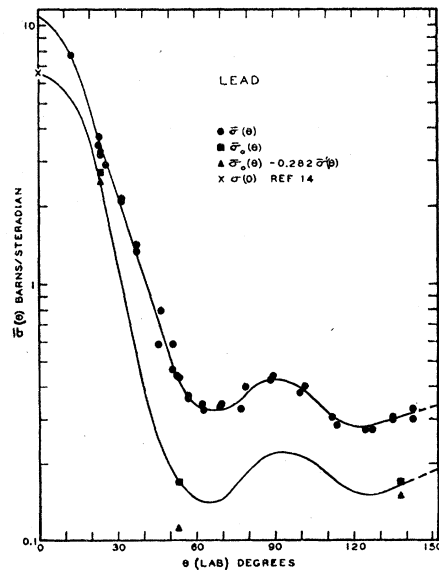


FIG. 8. Angular distribution of 3.7-Mev neutrons scattered from lead. Other remarks in caption of Fig. 6 apply here also.

¹¹ Nuclear Data, Natl. Bureau Standards Circ. 499 (U. S. Government Printing Office, Washington, D. C., 1950).

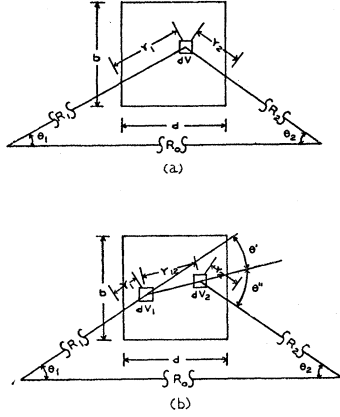


FIG. 9. Detail of scattering geometry: (a) single scattering; (b) double scattering.

APPENDIX I. SCATTERING OF NEUTRONS THROUGH RING SCATTERER BY SINGLE SCATTERING

In general the scattering ratio is made up of a sum of terms $S = S_1 + S_2 + \dots$, where S_1, S_2 , etc., refer to the neutrons scattered into the detector by single scattering, double scattering, etc. For the single scattering case [Figs. 1 and 9(a)] we have

$$S_1 = \int_V [I(\theta_1)/I(0)] \cdot [R_0^2/R_1^2 R_2^2] \cdot \sigma(\theta) n \cdot \exp[-\sigma n(r_1 + r_2)] \cdot A(\theta_2) E(E_n) dV. \quad (3)$$

The geometry is such that only small errors will be introduced if Eq. (3) is replaced by

$$S_1 = [I(\theta_1)/I(0)] \cdot [R_0^2/R_1^2 R_2^2] \cdot \sigma(\theta) n A(\theta_2) E(E_n) V F(\theta_2) \exp(-\sigma n d), \quad (4)$$

where

$$F = V^{-1} \int_V \exp[-\sigma n(r_1 + r_2 - d)] dV, \quad (5)$$

and the mean angles and distances are used for $\theta_1, \theta_2, R_0, R_1$, and R_2 . For a fixed size of ring scatterer, the quantity F is a function of θ_1 and θ_2 . However, since θ_1 only varies from about 5° to 15° , little error and much simplification is introduced by computing F for $\theta_1 = 0$. For the rectangular cross section of our scatterer, the integral F may be evaluated in terms of elementary functions. The results are displayed in Fig. 2.

If only single scattering were present, the quantity S_1 could be replaced by the measured data S and the differential cross section $\sigma(\theta)$ could be calculated. In any case the reduction of the data is facilitated by defining an effective single scattering differential cross section $\bar{\sigma}(\theta)$ such that

$$S = [I(\theta_1)/I(0)] \cdot [R_0^2/R_1^2 R_2^2] \cdot \bar{\sigma}(\theta) n A(\theta_2) E(E_n) V F(\theta_2) \exp(-\sigma n d). \quad (6)$$

APPENDIX II. SCATTERING OF NEUTRONS THROUGH RING SCATTERER BY DOUBLE SCATTERING

Using the quantities defined in Figs. 1 and 9b, the double scattering ratio is seen to be

$$S_2 = \int_{V_1} \int_{V_2} [I(\theta_1)/I(0)] \cdot [R_0^2/R_1^2 r_{12}^2 R_2^2] \cdot \sigma(\theta') \sigma(\theta'') n^2 \exp[-\sigma n(r_1 + r_{12} + r_2)] \times A(\theta_2) E(E_n) dV_1 dV_2. \quad (7)$$

An analytical solution of this integral seems quite involved, if not hopeless, for the geometry of the ring scatterer. In order to get some feeling for the manner in which the double scattering varies with the thickness of the ring, we have chosen to calculate the straight-through double scattering from a right circular cylinder assuming isotropic scattering [$\sigma(\theta') = \text{const} = \sigma/4\pi$]. In order to simplify this case as much as possible, let the neutron beam, incident on the circular end of the cylinder, be parallel to the cylinder axis, and let the detector sensitivities $A(\theta_2) = E(E_n) = 1$. Also let $r_1 + r_2$ be replaced by an approximate mean value d , the thickness of the cylinder. Equation (7) then reduces to

$$S_2 \equiv [\sigma^2 n^2 / 16\pi^2 R_2^2] \cdot \exp(-\sigma n d) \times \int_{V_1} \int_{V_2} r_{12}^{-2} \exp(-\sigma n r_{12}) dV_1 dV_2. \quad (8)$$

If the exponential function is expanded and the first three terms retained, S_2 reduces to the following:

$$S_2 = [\sigma^2 n^2 a^4 / 16R_2^2] \cdot \exp(-\sigma n d) \cdot (X - \sigma n a Y + \frac{1}{2} \sigma^2 n^2 a^2 Z), \quad (9)$$

where

$$X = -2(d^2/a^2) \cdot \ln d/a + 2(d^2/a^2) \sinh^{-1} d/2a + \cosh^{-1}(1 + d^2/2a^2) + 2d^2/a^2 - d^4/4a^4 - (1 - d^2/2a^2) \cdot [(1 + d^2/2a^2)^2 - 1]^{1/2}, \quad (10)$$

$$Y = 8 \int_0^\infty [xd/2a - \exp(-xd/2a)] \times \sinh(xd/2a) J_1(x) \sin x \cdot dx/x^4, \quad (11)$$

and

$$Z = d^2/a^2. \quad (12)$$

The integration of X was facilitated by the use of a theorem in vector analysis.¹² The integration of Y can be effected by recognizing that the integral corresponds to the electrostatic energy of a uniform volume distribution of charge.¹³

If the single scattering ratio S is calculated for the right circular cylinder under the same assumptions, then

¹² H. B. Phillips, *Vector Analysis* (John Wiley and Sons, Inc., New York, 1933), Chap. III.

¹³ W. R. Smythe, *Static and Dynamic Electricity* (McGraw-Hill Book Company, Inc., New York, 1939), Chap. V.

the effective single scattering cross section is given by

$$\bar{\sigma}/\sigma = 1 + (\sigma na/4)G(d/a), \quad (13)$$

where

$$G(d/a) = (a/d)(X - \sigma naY + \frac{1}{2}\sigma^2 n^2 a^2 Z) \quad (14)$$

and is written only as a function of d/a since it varies but slowly with σna , as may be seen in Fig. 4. By considering the mean curve to apply to all cases of interest, the function G becomes a function of d/a only.

To apply the calculations of the right circular cylinder to the case of the ring scatterer, we assume that except for multiplying factors which are angular functions,

the geometrical variation of the single and double scattering ratios is given correctly after associating the radial thickness of the ring scatterer b with the radius of the cylinder a .

If, instead of isotropic scattering, one takes the other extreme of an angular distribution peaked strongly in the forward direction, one finds that the single scattering ratio in the ring scattering varies as $d \exp(-\sigma nd)$ whereas the double scattering ratio varies as $d^2 \exp(-\sigma nd)$; thus leading to a linear variation of the apparent single scattering cross section with the thickness of the ring.

The Radioactive Decay of Tungsten 181†

J. M. CORK, W. H. NESTER, J. M. LEBLANC, and M. K. BRICE
Department of Physics, University of Michigan, Ann Arbor, Michigan
 (Received June 29, 1953)

Using tungsten enriched in mass 180, neutron capture produces a strong activity in W^{181} with a half-life of about 140 days. Using scintillation crystal and photographic magnetic spectrometers, two gamma rays of energy 136.5 and 152.5 kev are found to occur. Neither of these had been previously observed and conversely none of the previously reported gamma energies are found to exist. The main decay of W^{181} takes place by K capture directly to the ground state of Ta^{181} . Coincidence measurements are made with some evidence that the gamma rays are in sequence.

ON bombarding tantalum with high-energy (16-Mev) deuterons, Wilkinson found¹ that a radioactive tungsten of half-life 140 days could be chemically separated from the target. Since natural tantalum consists only of mass 181, the $(d,2n)$ reaction could produce W^{181} . The more common (d,n) process would result in W^{182} , which is stable in nature. A similar radioactive tungsten product was later produced² by bombarding tantalum with protons, thus inducing the reaction $Ta^{181}(p,n)W^{181}$. Since the natural relative abundance of W^{180} is only 0.13 percent, the neutron capture process in the pile with ordinary tungsten is not highly productive of W^{181} . Its presence, however, has been observed by this method and certain values ascribed³ to the energies of its gamma rays.

In the present investigation a specimen of tungsten with a fifty-fold enrichment in mass 180 was kindly made available by the Oak Ridge National Laboratory. Samples were irradiated for a two-month period in both the Oak Ridge and the Argonne piles. In addition to the long-lived W^{181} , a rather strong yield of the well-

known⁴ short-lived W^{187} was obtained, as well as a certain amount of the 73-day W^{185} , which emits only beta radiation.

A study of the radiations from the long-lived W^{181} has been made, utilizing magnetic photographic spectrometers to observe conversion and photoelectrons and the scintillation crystal spectrometer for any unconverted gamma rays and coincidence events. In addition to several Auger electron lines, five conversion electron lines are found with energies of 69.0, 85.0, 125.0, 141.0, and 149.8 kev. These form a $K-L$ and a $K-L-M$ group for gamma energies of 136.5 and 152.5 kev. The K conversion lines for the two gamma rays are about of equal intensity and the K/L ratio for each is, by visual estimate, approximately 8 ± 2 .

A survey of the high-energy gamma spectrum to detect the previously observed gamma energies was made with the scintillation crystal spectrometer. No evidence could be found for a gamma ray as reported¹ at 1.8 Mev nor for energies of 30, 600, and 800 kev as found³ by Alburger *et al.* The peak due to the tantalum x-rays is extremely strong, and had any of the other unconverted gamma rays been as much as one-millionth as intense they could have been detected. A spectrographic analysis of the enriched tungsten specified a high purity, with zinc present to no greater than 0.01

† This project received the joint support of the U. S. Office of Naval Research and the U. S. Atomic Energy Commission.

¹ G. Wilkinson, *Nature* **170**, 864 (1947).

² J. Burkig and J. Richardson, *Phys. Rev.* **76**, 586 (1949).

³ Alburger, der Mateosian, Friedlander, Goldhaber, Mihelich, Scharff-Goldhaber, and Sunyar, Brookhaven National Laboratory Quarterly Progress Report, July 1-September 30, 1950, p. 2 (unpublished).

⁴ Cork, Brice, Nester, LeBlanc, and Martin, *Phys. Rev.* **89**, 1291 (1953).